Proc. Natl. Acad. Sci. USA
Vol. 96, pp. 945–949, February 1999
Cell Biology

Multiple and diverse forms of regulated exocytosis in wild-type and defective PC12 cells

HARUO KASAI*, TAKUYA KISHIMOTO*, TING-TING LIU*, YASUSHI MIYASHITA*, PAOLA PODINI†, FABIO GROHOVAZ†, AND JACOPO MELDOLESI†‡

*Department of Physiology, University of Tokyo, Bunkyo-ku, Tokyo 113, Japan; and †Department of Pharmacology, B. Ceccarelli Center, University of Milan, Center of Cellular and Molecular Pharmacology, Consiglio Nazionale delle Ricerche, and DIBIT, Scientific Institute S. Raffaele, Via Olgettina 58, 20132 Milan, Italy

Communicated by George E. Palade, University of California, San Diego, La Jolla, CA, November 30, 1998 (received for review December 12, 1997)

ABSTRACT **Regulated exocytosis triggered by the photolysis of a caged Ca^{2+} compound, DM-nitrophen, was investigated by patch-clamp capacitance measurements in two clones of PC12, the first wild-type and the second (PC12-27) defective of both types of classical secretory vesicles together with the neuronal-type receptors for the attachment proteins of the N-ethylmaleimide-sensitive fusion protein, the so called SNAREs. Moreover, the electrophysiological data were correlated with the ultrastructure of resting quick-frozen–freeze-dried cells of the two clones. Wild-type PC12 exhibited two-component capacitance responses, time constants of 30–100 ms and >10 s, that previous studies had suggested to reflect primarily the fusion of the small and large secretory vesicles, each contributing cell surface increases of ≈10%. Both of these components were largely and specifically inhibited whether cells previously were microinjected with tetanus toxin light chain. In the defective clone, large responses also were recorded (≈19% surface expansion; time constant, ≈1 s) that, in contrast to those of the wild-type, were entirely resistant to the toxin. Although secretory organelles, i.e., large vesicles and also profiles of small vesicles, were abundant at the cell periphery and often docked to the plasmalemma of resting wild-type PC12, in the defective clone, no superficial accumulation of vesicles was observed. Our coordinate structural and functional results have revealed diversities between the two classical forms of regulated secretion in wild-type PC12 and have provided evidence of a toxin-insensitive form of Ca^{2+}-induced exocytosis, prominent in the defective clone, that may play an important role(s) in cellular physiology.**

Regulated secretion has been shown to take place in neurosecretory cells by the exocytic discharge of two types of organelles, the large (or dense-core) and the small (or synaptic-like) vesicles (LVs and SVs, respectively; ref. 1, 2). In spite of the specificity of their cargoes and of their intracellular pathways, these organelles share part of their membrane components, and their exocytosis is mediated by the same v and tSNARE (a receptor for the attachment proteins of the *N*-ethylmaleimide-sensitive fusion protein) system (3–6). As a consequence, discharge of both of these vesicles is blocked by chlostridial toxins, the tetanus (TeTx) and botulinum toxins, working as endopeptidases specific for either the vesicle VAMP-2 or the plasmalemma syntaxin 1A and SNAP-25 SNARE proteins (7). Whether LVs and SVs represent the only organelles competent for regulated exocytosis is still debated. Patch clamping and biochemical studies carried out with appropriate rises of the cytosolic free Ca^{2+} concentration, $[Ca^{2+}]_i$, also from cells widely considered nonsecretory, such as Chinese hamster ovary and other fibroblast lines, have in fact provided evidence of increased exocytic discharge (8–10). Moreover, in chromaffin cells, the combination of patch clamping with amperometry has revealed, in addition to the catecholamine release responses, an additional capacitance increase component sustained by a toxin-insensitive form of exocytosis whose underlying organelles have remained unidentified (11). At the moment, the existence in neurosecretory and other types of cells of new, regulated exocytic pathway(s) represents, therefore, an exciting possibility.

In the present work, regulated secretion has been investigated in PC12, a rat pheochromocytoma line that offers distinct advantages. On the one hand, PC12 secretory organelles, LVs, and SVs are well known because of extensive evidence accumulated by microscopy, immunocytochemistry, and subcellular fractionation as well as biosynthesis and secretion studies (12–14). Moreover, the application to PC12 of patch-clamp capacitance recordings has led to the identification of the exocytic properties of these organelles, revealing, in particular, differences in time constants and $[Ca^{2+}]_I$-dependence (15, 16). On the other hand, expression of LVs and SVs is not a rule of PC12 because a defective clone is available (PC12-27) that, in spite of its largely maintained phenotype, lacks both of the classical neurosecretory organelles (17). By the parallel investigation of wild-type and defective PC12 cells, carried out by capacitance recording and electron microscopy of quick-frozen–freeze-dried (qf-fd) cells, we have clarified various aspects of the neurosecretory processes from PC12 and have demonstrated that a Ca^{2+}-induced and TeTx-insensitive exocytic pathway really exists and is predominant in the PC12-27 clone.

MATERIALS AND METHODS

Capacitance Measurements. Capacitance measurements were performed in whole-cell patch-clamped cells as described (15). In brief, a 1-kHz sine-wave voltage command with a peak-to-peak amplitude of 100 mV was superimposed on the holding potential of 0 mV. In most of the experiments, membrane capacitance was calculated from 10 cycles of sine waves and was sampled at 83 Hz; in others, it was calculated from one cycle of sine waves and was sampled at 1 kHz. The internal solution contained (in mM): 50 Cs-Hepes (pH 7.2), 100 Cs-glutamate, 5 CsCl, 0.2 benzothiazole coumarin (Molecular Probes), and 10 mM dimethoxynitrophenamine tetrasodium salt (DM-nitrophen, Calbiochem) together with 0.5–4 mM $CaCl_2$. Membrane capacitance of PC12 clone cells, wild-

The publication costs of this article were defrayed in part by page charge payment. This article must therefore be hereby marked "*advertisement*" in accordance with 18 U.S.C. §1734 solely to indicate this fact.

PNAS is available online at www.pnas.org.

Abbreviations: LV, large vesicle; SV, small vesicle; TeTx, tetanus toxin; qf-fd cells, quick-frozen–freeze-dried cells; ER, endoplasmic reticulum.

‡To whom reprint requests should be addressed at: DIBIT, Scientific Institute S. Raffaele, Via Olgettina, 58, 20132 Milan, Italy. e-mail: meldolesi.jacopo@hsr.it.

type PC12-B7 (15, 16), and defective PC12-27 (17) was 13.2 ± 4.2 and 16.4 ± 8.6 pF (mean ± SD; n = 205 and 65), respectively. Mean access resistance was 8.5 ± 1.5 megaohms.

$[Ca^{2+}]_i$ Measurement and Photolysis of the Caged-Ca^{2+} Compound. Dual-wavelength fluorimetric Ca^{2+} assays were performed as described by using the ratiometric long-wavelength indicator benzothiazole coumarin (15). In brief, the dye was excited with light emitted from a xenon lamp alternated rapidly between 430 and 480 nm (TILL Photonics, Planegg, Germany), and the emitted fluorescence, collected through the objective lens, was passed through an LP520 filter and was detected by using a photomultiplier (NT5783, Hamamatsu Photonics, Hamamatsu City, Japan). Photolysis of the caged-Ca^{2+} compound, DM-nitrophen, was performed by using a xenon flash lamp (High-Tech Instruments, Aberdeen, U.K.).

Microinjection of Tetanus Toxin. TeTx light chain [recombinant, 0.1 mg/ml dissolved in a solution containing, in mM, 150 NaCl and 10 Na-Hepes (pH 7.4)] was injected into PC12-B7 and PC12-27 cells under an inverted microscope by using an automatic microinjector (Eppendorf 5246). The injection solution also contained (in mM) 0.1 fura-2-dextran (Molecular Probes). The final toxin concentration was estimated at ≈20 nM. Sham injection was made by replacing the same amount of TeTx with BSA (Sigma). The injected cells, identified by the fluorescence of fura-2, were whole-cell clamped and investigated as described above after a 2- to 5-hr rest in the CO_2 incubator.

Microscopy. Cutaneous pectoris muscles from the frog and PC12 cell monolayers (wild-type B7 and defective 27 clones), grown over small plastic dishes, were prepared as described in refs. 18 and 19, respectively, and were quick-frozen by propulsion against a liquid helium-cooled copper block. Frozen specimens were transferred into an ultra-high-vacuum chamber (Cryofract 190, Reichert-Jung) and were freeze-dried under controlled conditions. At the end of the drying cycles (3–4 days), when pressure and temperature were restored to room values, the specimens were removed from the vacuum apparatus, were exposed overnight to OsO_4 vapors, and then were embedded in Araldite. Thin sections were cut with a diamond knife in a Reichert-Jung Ultracut microtome, were collected on uncoated grids, were stained with uranyl acetate and lead citrate, and were examined in a Hitachi H7000 (Hitachi, Tokyo) electron microscope. Countings of membrane profiles were performed on groups of randomly chosen photographs printed at the same final magnification (50,000×). Morphometric analyses were carried out according to Weibel *et al.* (20).

For immunofluorescence and immunogold staining, unfixed qf-fd specimens were embedded at −20°C in Lowicryl K4. Ultrathin sections then were exposed for 1 hr at room temperature to the appropriately diluted first antibody and then were washed and treated with anti-Igs, either labeled with rhodamine or attached to 5-nm gold particles. After further washing, the sections were fixed with 1% OsO_4, were stained, and were examined as described above. For further details, see ref. 19.

RESULTS

Patch-Clamp Capacitance. Regulated exocytosis was triggered in patch-clamped PC12 cells by photolysis of the caged Ca^{2+} compound, DM-nitrophen (see ref. 14). Such an approach induces a rapid and homogeneous $[Ca^{2+}]_i$ elevation and therefore guarantees that organelles, no matter of their intracellular localization, are simultaneously exposed to the same high concentration of the cation (8, 11, 15, 16, 21). The cell surface increases revealed by capacitance measurements in wild-type PC12 cells fully competent for regulated exocytosis of both SVs and LVs, (clone B7, >100 cells analyzed) were in line with previous data (15, 16). Two increases appeared in sequence, distinct from each other in terms of timing and kinetics, and each were followed by a decline documenting membrane recycling from the surface (Fig. 1*A*). The first component, which included discharged SVs (16) and required $[Ca^{2+}]_i$ increases of >10 μM, began after a short delay (≈10 msec) and was approximated by an exponential function with a time constant of ≈30–100 msec (15); the second, a catecholamine discharging component with much slower kinetics (time constant >10 sec), featured a higher affinity for Ca^{2+} and a slower decline (LV in Fig. 1 *A* and *E*; see ref. 16). The two capacitance rises of the wild-type clone were recalculated in terms of cell surface expansion and were found to correspond to roughly similar values (13 ± 5 and 10 ± 7% of the resting plasmalemma; Table 1).

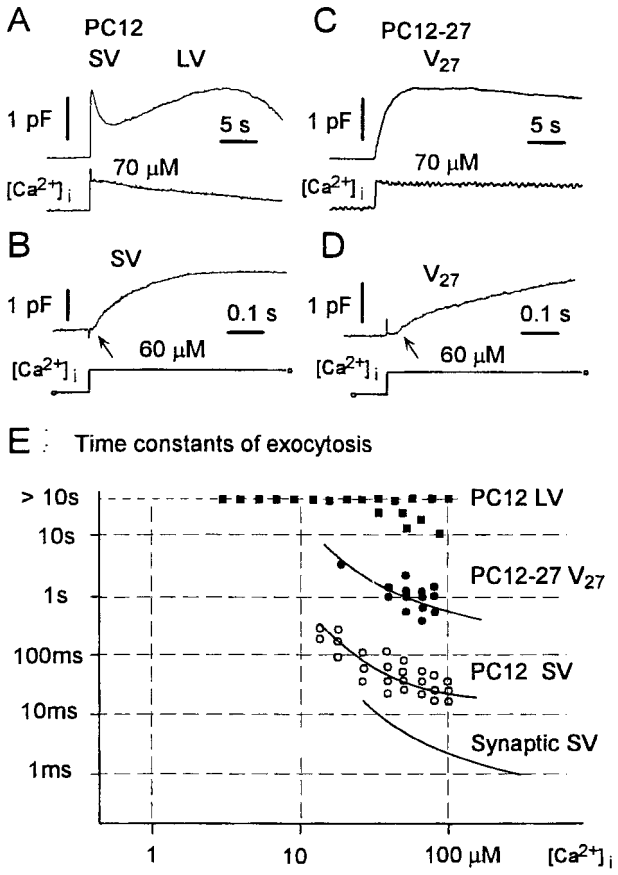

FIG. 1. Capacitance measurements of exocytosis induced by photolysis of the caged compound DM-nitrophen in wild-type PC12 (*A* and *B*) and defective PC12-27 (*C* and *D*) cells. (*A* and *C*) Capacitance changes displayed in a compressed time scale. Lower traces indicate $[Ca^{2+}]_i$ measured by using the fluorescent dye benzothiazole coumarin. Wild-type PC12 cells (*A*) show the typical pattern composed by fast and slow exocytoses, each of which is followed by recycling. SV and LV labeling refers to predicted contribution of the corresponding vesicles. In contrast, PC12-27 cells (*C*) display mainly a single, slower response (V_{27}), not followed by fast recycling. (*B* and *D*) Capacitance increases recorded with a high time resolution in wild-type PC12 and PC12-27 cells, respectively. In the wild-type cell, the capacitance increase begins after a short delay (≈10 msec; arrow in *B*). This increase is approximated by using an exponential function with a time constant of 60 msec. In PC12-27 cell, the capacitance increase becomes appreciable after ≈35 msec (arrow in *D*). The increase can be fitted by using the sum of two exponential functions with time constants of 44 msec and 1.1 sec, accounting for the 14 and 86% of the response in PC12-27, respectively. *E* illustrates the Ca^{2+} dependence and time constants of exocytoses in wild-type and defective PC12, compared with values in synapses. The smooth line for synaptic SV is from ref. 21.

Table 1. Surface expansion induced by the $[Ca^{2+}]_i$ rise after DM-nitrophen photolysis, and resting distribution of secretory organelles in wild-type and defective PC12 cells

	Wild-type PC12		PC12-27
	SV	LV	V_{27}
Cell capacitance*			
Surface expansion, percent ± SD of the resting plasmalemma	13 ± 5.1%	10 ± 7.1%	19.1 ± 8.8%
Vescicle morphometry, number per square micrometer and percent surface correspondance to the resting plasmalemma†			
Docked	3.2 ± 1.1, 2.5%	5.2 ± 0.8, 18.1%	0.5 ± 0.2, 0.4%
In the juxtaplasmalemma layer, 0.5 μm thick	15.3 ± 2, 12.0%	2.6 ± 0.2, 8.9%	5.3 ± 0.8, 4.2%

*Surface expansion of resting wild-type and defective PC12 cells was assessed directly from capacitance measurements. V_{27} in the PC12-27 column refers to the sum of the two capacitance components with time constants of ~50 msec and 1 sec observed in the defective clone.

†SV, LV, and V_{27} profiles were counted in groups of pictures from qf-fd samples of PC12 and PC12-27 cells printed at 50,000×. LVs were recognized easily because of their peculiar features; their diameter, as established from measurements in a group of 55 organelles that appear equatorily sectioned, was 105 ± 5 nm. Profiles taken for SVs and V_{27} were discrete, round, or moderately elongated, with dense content and transverse size varying from 40 to 60 nm. Inclusion in the population of transverse sections of tubules (ER, endosomes) could not be excluded. Profiles given as docked appeared in contact with the plasmalemma, either directly or via short bridges. The overall length of the cell profile investigated amounted to 227 and 95 μm for wild-type PC12 and PC12-27, respectively. The number of vesicles per cell surface area was calculated from the data of electron micrographs as recommended by Weibel *et al.* (20), assuming the average section thickness to be 45 nm. Correspondance of vesicle cumulative surface to the resting plasmalemma was calculated assuming the average surface of single SV and V_{27}, on the one hand, and LV, on the other hand, to be 7,850 and 35,000 nm^2, respectively.

Both Ca^{2+}-induced capacitance responses of wild-type PC12 cells were profoundly and consistently reduced after microinjection with the TeTx light chain (13 cells; Fig. 2 *A* and *B*). Under the latter conditions, the initial rise was on the average of only 6.6 ± 1% of the cell surface, corresponding to an ≈50% reduction with respect to controls, and the second component was affected even more severely (calculated rate was 0.15 ± 0.15%/sec, i.e., ≈14% of controls). Moreover, the reductions were accompanied by evident slowing down of the responses (time constant of the first component was 450 ± 65 msec). The specificity of the TeTx-induced changes was demonstrated by the results in the sham-injected cells (n = 14), in which no major changes were observed. In fact, the initial increase was on the average of 12 ± 2% with a time constant of 90 ± 25 msec, and the second increase (slope at 10 sec) was 0.75 ± 13%/sec, i.e., ≈92 and 70% of controls, respectively.

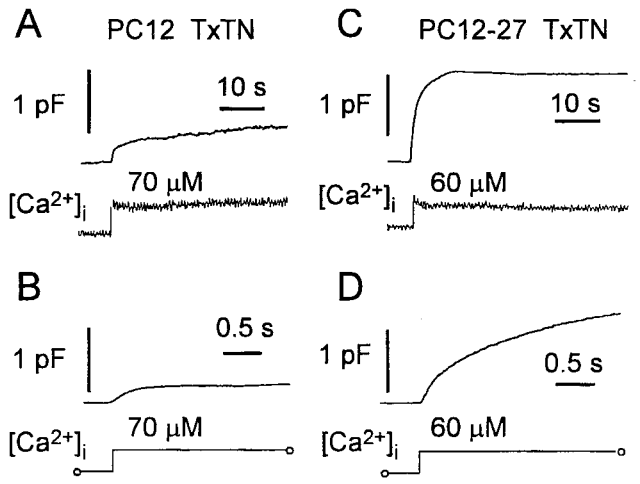

FIG. 2. Capacitance measurements of exocytosis induced by photolysis of the caged compound DM-nitrophen in TeTx-treated wild-type PC12 (*A* and *B*) and defective PC12-27 (*C* and *D*) cells. *A–D* match the corresponding panels of Fig. 1. From the comparison of the figures emerges a marked decrease of both the fast and slow components and the slowing of the fast component in the wild-type cells (compare Fig. 2*A* to Fig. 1*A*). In contrast, no change of the capacitance responses was detected in PC12-27 cells (compare Fig. 2*C* to Fig. 1*C*). From the initial capacitance increases recorded with high time resolution (*B* and *D*; cells shown are different from those in *A* and *B*), the time constant in the wild-type PC12 was approximated to 410 msec. In the PC12-27 cell, the increase could be fitted by using the sum of two exponential functions with time constants of 68 msec and 1.1 sec, comprising ≈20 and 80% of the response, respectively.

Experiments parallel to those reported so far were carried out with cells of the defective PC12-27 clone. Previous reports (17, 22) had shown these cells to exhibit a host of neurosecretory markers typical of PC12, including Ca^{2+} channels, receptors, and G proteins. In contrast, LVs could not be seen by electron microscopy, and the molecular components of both the latter organelles and SVs, as well as the plasmalemma tSNAREs, remained undetectable by Western blotting and immunofluorescence. Taken together, these results qualify PC12-27 as neurosecretory cells incompetent for regulated exocytosis (17). In spite of the cellular and molecular defects, photolysis of DM-nitrophen induced in PC12-27 cells large capacitance responses after a delay (35 msec) only moderately longer than that preceding the fast response in the wild-type clone (Fig. 1, compare *C* and *D* to *A* and *B*). As in the latter, the capacitance rise in the defective clone cells was smooth (Fig. 1*D*), documenting the Ca^{2+}-regulated exocytosis of small surface organelles (indicated from here on as V_{27}). A major difference with respect to wild-type cells emerged in contrast with time. In most PC12-27 cells, the capacitance increase did not stop but kept increasing, although at slow rates, for periods up to several tenths of a second. In other cells, however, slow declines became evident 5–10 sec after the $[Ca^{2+}]_i$ rise (Figs. 1*C* and 2*C*). In terms of surface expansion, the single capacitance rise of clone 27 approximated the sum of the two rises in the wild-type cells (19.1 ± 8.8%; Table 1); in terms of $[Ca^{2+}]_i$-dependence, it was not significantly different from the SV peak of the wild-type (Fig. 1*E*); in terms of kinetics, it could be fitted by the sum of 2–3 exponential functions, the major of which (70–80%) with time constant of 1.1 sec (Fig. 1*D*). When PC12-27 were microinjected, significant changes of the capacitance responses were observed neither in the sham nor in the TeTx-treated cells (analyzed cells 7 and 8; in Figs. 1 and 2, compare *C* and *D*). In particular, in poisoned cells, the average capacitative response of V_{27} amounted to 14 ± 3.7%, and the time constant amounted to 1.2 ± 0.26 sec (76 and 108% of uninjected PC12-27). When the minor early component calculated in the PC12-27 response was considered, its properties also were found to remain unchanged after TeTx. Total surface cell rise was, in fact, 2.2 ± 0.4% (vs. 2.5%), with a time constant of 58 ± 12 msec (vs. 65 msec).

Electron Microscopy. In the present, work the cells were processed by qf-fd, a physical fixation–dehydration procedure, instead of the most widely used chemical fixation followed by dehydration with organic solvents. This choice was made

because, during chemical fixation, exocytosis as well as fusion of vesicles with cytoplasmic organelles may take place (23–25) followed, during dehydration, by extensive extraction and redistribution of cell components (14, 26, 27), with ensuing uncontrolled changes of membrane compartments.

To establish identification criteria for bona fide secretory organelles that had been processed by the qf-fd procedure, a frog neuromuscular preparation (24) was investigated first. As can be seen in Fig. 3*A*, the SVs within the nerve terminals exhibited the classical size (≈50 nm) and distribution in clusters, with the superficial layers apposed (docked), directly or via a short bridge, to the presynaptic plasmalemma (Fig. 3*A Inset*). Compared with their chemically fixed counterparts, the profile of these SVs appeared more irregular, and their lumen was much more dense (Fig. 3*A*), most likely because artifactual extraction of their content had been prevented.

The results obtained by qf-fd of wild-type PC12 cells are shown in Fig. 3 *B–E*. Recognition and counting of the profiles with SV and LV appearance revealed specific aspects different from those at synapses. From a survey of numerous electron microscopical images of cross-sectioned cell profiles, ≈50% of the cell LVs was found apparently docked to the plasmalemma (see also ref. 28), and 25% was found undocked but positioned in the superficial, 0.5-μm-thick layer of cytoplasm. Of the SV profiles, only a relatively small fraction appeared docked whereas many more were free, distributed at random in the juxtaplasmalemma layer (Fig. 3 *C–E*; Table 1). The surface concentration of both types of secretory organelles in wild-type PC12 was confirmed by immunocytochemistry for vesicle membrane proteins [carried out by both immunofluorescence (data not shown) and high-resolution immunogold (see Fig. 3B for synaptophysin)].

When qf-fd PC12-27 cells were studied by electron microscopy (Fig. 4), LVs were confirmed to be completely absent (22) whereas only a few vesicular profiles appeared immediately

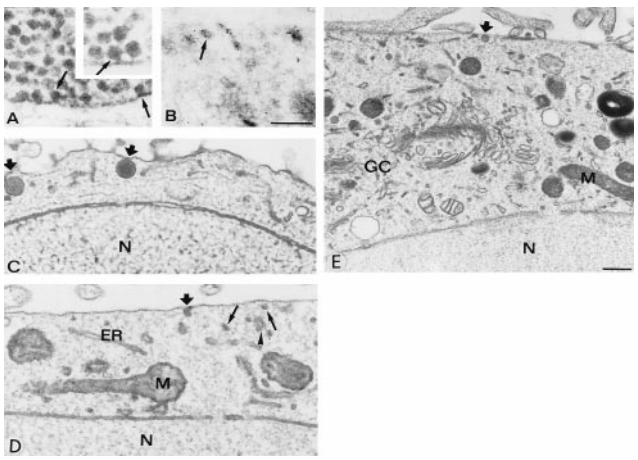

FIG. 3. Electron microscopy of a frog neuromuscular junction (*A*) and wild-type PC12 cells (*B–D*) physically fixed by qf-fd while at rest. *A* shows aggregation of synaptic SVs in the proximity or in direct contact [docking shown by arrows in the main panel as well as in the high magnification (*Inset*, ×100,000)] with the presynaptic plasma membrane. *B* shows a wild-type PC12 processed as described in ref. 18, immunogold-labeled for synaptophysin, a protein of SV (arrow) membranes. Additional immunolabeling decorates structures adjacent or perpendicular to the plasmalemma, most likely participating in endocytosis (13). *C–D* show images of wild-type PC12 cells illustrating the docking to the plasmalemma of two LVs (thick arrows in *C*) and of a single SV (thick arrow in *D*), with additional SV profiles (arrows) present in the juxtaplasmalemma layer of the cytoplasm; the arrowhead points to a cluster of apparently interconnected profiles, possibly of ER nature. *E* shows a vast cytoplasmic area including the section of the Golgi complex (GC) and trans-Golgi network. A docked LV is pointed by the thick arrow. N, nucleus; M, mitochondrion. [Bars = 0.3 μm (*A–D*).] Morphometry of data is reported in Table 1.

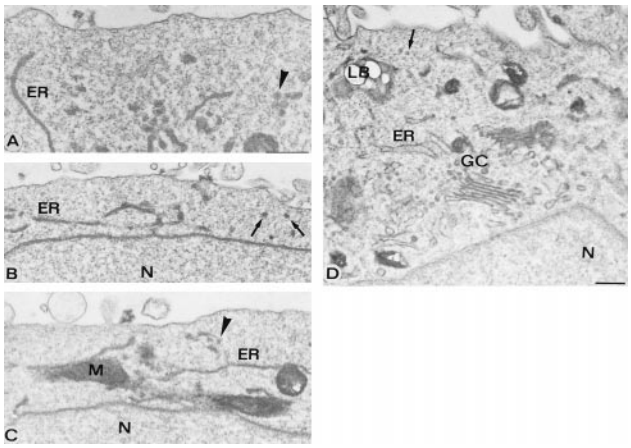

FIG. 4. Electron microscopy of defective PC12-27 cells physically fixed by qf-fq while at rest. Notice that, in all panels, the cytoplasmic layer adjacent to the plasmalemma is almost completely devoid of vesicles profiles. In contrast, profiles are numerous in the deeper layers of the cytoplasm in which other organelles (mitochondria and ER cisternae) are also visible. Profiles that might be V_{27} are pointed out by arrows, and those that might be ER clusters are pointed out by arrowheads. A well developed Golgi complex (GC), with its adjacent trans-Golgi network, shows a large complement of vesicles (*D*). [Bars = 0.3 μm (*A–C*).] N, nucleus; M, mitochondrion; LB, lipid body. Morphometry is reported in Table 1.

adjacent to the plasmalemma and were distributed in the superficial cytoplasmic layer (on the average, the profiles were $<1/3$ the density in the wild-type clone; compare Fig. 4 *A–D* to Fig. 3 *C–E*, and see Table 1). Defects of the PC12-27 clone were not general throughout the cell. In fact, vesicle profiles at some distance from the surface were abundant (Fig. 4 *A–D*), similar to the wild-type clone. Also similar were the long endoplasmic reticulum (ER) cisternae distributed throughout the cytoplasm, including the juxtaplasmalemma layer (Figs. 3 *C–E* and 4 *A–D*), as well as the organelles located deep in the cytoplasm, including the Golgi complex and the trans-Golgi network. In the latter structures, the density of vesicles was prominent, similar to both the wild-type and the PC12-27 clone cells (Figs. 3*E* and 4*D*).

DISCUSSION

Taken together, our electrophysiological and ultrastructural results confirm and expand the present information about diversity in Ca^{2+}-dependent exocytosis. Three aspects of our experiments deserve attention. First, photolysis of a cytosolic caged Ca^{2+} compound does expose all secretory vesicles to the same $[Ca^{2+}]_i$ jump, no matter their intracellular distribution. Second, during whole-cell perfusion, no MgATP was included in the patch pipette. Thus, exocytoses revealed by capacitance measurements could only result from organelles that, at the moment of the trigger by Ca^{2+}, had already been ATP-primed for discharge (in this respect, see also refs. 15, 21, and 29). Finally, our ultrastructural studies were conducted on cells that had been quick-frozen and then freeze-dried before fixation and embedding (18, 19). This elaborate procedure was used to prevent artifactual membrane redistributions that may take place with conventional fixations (14, 26, 27).

Of the two types of secretory organelles known to exist in the wild-type PC12 (12–16), only LVs can be identified easily by conventional electron microscopy. The surface distribution of these organelles, with extensive docking to the plasmalemma (28), was confirmed in the qf-fd cells. Thus, the slow rate of their triggered exocytosis cannot be attributable to their intracellular migration but rather reflect specific properties of the LV membrane fusion in the PC12 system (see refs. 16 and

30). As far as SVs, it should be emphasized that, in the electron microscope, these organelles cannot be distinguished from other small vesicular profiles unless specifically immunolabeled. Thus, the values for docked and membrane-adjacent profiles provided for SVs in Table 1 are most likely in excess with respect to the distribution of these organelles in resting PC12. Nevertheless, these values remain largely below those expected from the fast capacitance increases, strongly suggesting that, for most of the rapidly fused SVs, the preexocytic interaction with the plasmalemma takes place during, and not before, the Ca^{2+} trigger.

The Ca^{2+}-triggered capacitative response of wild-type PC12 was reduced greatly by TeTx, especially in its LV component, whereas the fast component became slower. Indeed, during chlostridial toxin poisoning, discharge of individual secretory vesicles is known to be slowed down before blockade (7, 11). It is, therefore, possible that the slower response visible in poisoned wild-type PC12, illustrated in Fig. 2 *A* and *B*, is sustained, at least in part, by toxin-sensitive vesicles, especially SVs. It should be noted, however, that its kinetics resembles that of the TeTx-insensitive response sustained by V_{27} in the defective PC12-27 clone cells. It is suggested, therefore, that the latter vesicles exist also in wild-type cells to an extent, however, inappreciable by capacitance measurements unless the contribution of SVs and LVs is largely cut down by TeTx.

Previous biochemical studies showed that PC12-27 cells lack the classical chlostridial toxin-sensitive SNAREs responsible for regulated exocytic fusion of SVs and LVs (17). Other SNAREs, possibly active within the cell as well as at its plasmalemma (6), may, however, be expressed in PC12-27. It was, therefore, consistent to find that the defective cells, although exhibiting a regulated secretion activity, are unaffected by TeTx. The toxin-resistant activity appears to be sustained by vesicles (V_{27}) whose existence up to now had not even been envisaged. The slower kinetics of their discharge (with respect to SV) might be attributable to their scattered distribution within the cell. Because PC12-27 cells release neither acetylcholine nor catecholamines and chromogranins (17, 22), the role of V_{27} may not be in cargo discharge. Instead, these vesicles may serve in membrane addition for the sealing of plasmalemma lesions (31, 32) and/or for the transfer to the cell surface of integral membrane proteins such as channels, receptors, and transporters. In many cells, including PC12 cells (33), proteins of that type are known to shuttle between surface and internal membranes; however, the nature of their transport vesicles has not been identified yet.

In conclusion, the coordinate functional and structural results we have obtained have yielded information, on the one hand, on the classical forms of regulated exocytosis of wild-type PC12 cells and, on the other hand, on a TeTx-insensitive form that accounts for the bulk of the Ca^{2+}-induced exocytic responses in the defective PC12-27 clone. Such a form could be present, although to a much lower level, also in the wild-type cells. The kinetic properties of its discharge resemble those reported in cells believed until recently to be incompetent for regulated exocytosis, such as Chinese hamster ovary and other fibroblast lines (8, 9). Moreover, an exocytic component, which seems to resemble the system of PC12-27 in both its relatively slow kinetics (time constants of 1.1–6.4 vs. 1.1 sec) and toxin resistance, has been described very recently in chromaffin cells (11). Taken together, these findings strongly suggest regulated exocytosis to include several and diverse routes, calling attention to cell models such as the PC12 and its defective PC12-27 clone which, because of their favorable properties, could become instrumental for further development of knowledge in the field.

We thank Drs. Philip Washbourne and Cesare Montecucco for the kind gift of recombinant TeTx light chain. This work was supported by Grants-in-Aid from the Japanese Ministry of Education, Science and Culture; the Italian Ministry for Research and University; the Takeda Foundation; the Armenise–Harvard Foundation; the Human Frontier Science Program (Grant RG0520/1995M); Research for the Future of the Japan Society for the Promotion of Science; European Community Biotech Program; and Core Research for Evolutional Science and Technology of the Japan Science and Technology Corporation.

1. Kelly, R. B. (1991) *Curr. Opin. Cell Biol.* **3,** 654–660.
2. Kelly, R. B. (1993) *Cell* **72,** 43–53.
3. Rothman, J. E. (1994) *Nature (London)* **372,** 55–63.
4. Goda, Y. (1997) *Proc. Natl. Acad. Sci. USA* **94,** 769–772.
5. Hanson, P. I., Heuser, J. E. & Jahn, R. (1997) *Curr. Opin. Neurobiol.* **7,** 310–315.
6. Götte, M. & Fischer von Mollard, G. (1998) *Trends Cell Biol.* **8,** 215–218.
7. Montecucco, C. & Schiavo, G. (1995) *Q. Rev. Biophys.* **28,** 423–472.
8. Coorssen, J. R., Schmitt, H. & Almers, W. (1996) *EMBO J.* **15,** 3787–3791.
9. Ninomiya, Y., Kishimoto, T., Miyashita, Y. & Kasai, H. (1996) *J. Biol. Chem.* **271,** 17751–17754.
10. Chavez, R. A., Miller, S. G. & Moore, H.-P. H. (1996) *J. Cell Biol.* **133,** 1177–1191.
11. Xu, T., Binz, T., Niemann, H. & Neher, E. (1998) *Nat. Neurosci.* **1,** 192–200.
12. Clift-O'Grady, L., Linstedt, A. D., Lowe, A. W., Grote, E. & Kelly, R. B. (1990) *J. Cell Biol.* **110,** 1693–1703.
13. Baumert, M., Takei, K., Hartinger, J., Burger, P. M., Fischer von Mollard, G. Maycox, P. R., De Camilli, P. & Jahn, R. (1990) *J. Cell Biol.* **110,** 1285–1294.
14. Schmidt, A., Hannah, M. J. & Huttner, W. B. (1997) *J. Cell Biol.* **137,** 445–458.
15. Kasai, H., Takagi, H., Ninomiya, Y., Kishimoto, T., Ito, K., Yoshida, A., Yoshioka, T. & Miyashita, Y. (1996) *J. Physiol.* **494,** 53–65.
16. Ninomiya, Y., Kishimoto, T., Yamazawa, T., Ikeda, H., Miyashita, Y. & Kasai, H. (1997) *EMBO J.* **16,** 929–934.
17. Corradi, N., Borgonovo, B., Clementi, E., Bassetti, M., Racchetti, G., Consalez, G. G., Huttner, W. B., Meldolesi, J. & Rosa, P. (1996) *J. Biol. Chem.* **271,** 27116–27124.
18. Grohovaz, F., Bossi, M., Pezzati, R., Meldolesi, J. & Torri Tarelli, F. (1996) *Proc. Natl. Acad. Sci. USA* **93,** 4799–4803.
19. Pezzati, R., Bossi, M., Podini, P., Meldolesi, J. & Grohovaz, F. (1997) *Mol. Biol. Cell* **8,** 1501–1512.
20. Weibel, E. R., Gonzague, S. K. & Scherle, W. F. (1996) *J. Cell Biol.* **30,** 23–38.
21. Heidelberger, R., Heinemann, C., Neher, E. & Matthews, G. (1994) *Nature (London)* **371,** 513–515.
22. Clementi, E., Racchetti, G., Zacchetti, D., Panzeri, M. C. & Meldolesi, J. (1992) *Eur. J. Neurosci.* **4,** 944–953.
23. Heuser, J. E., Reese, T. S. & Landis, D. M. D. (1974) *J. Neurocytol.* **3,** 109–131.
24. Ceccarelli, B., Grohovaz, F. & Hurlbut, W. P. (1979) *J. Cell Biol.* **81,** 178–192.
25. Brewer, P. A. & Linch, K. (1986) *Neuroscience* **17,** 881–895.
26. Kellenberger, E., Johansen, R., Maeder, M., Bohrmann, B., Stauffer, E. & Villiger, W. (1992) *J. Microsc. (Oxford)* **168,** 181–201.
27. Chung, K. N., Elwood, P. C. & Heuser, J. E. (1996) *Mol. Biol. Cell* **7,** 277 (abstr.).
28. Banerjee, A., Kowalchyk, J. A., DasGupta, B. R. & Martin, T. F. J. (1996) *J. Biol. Chem.* **271,** 20227–20230.
29. Bruns, D. & Jahn, R. (1995) *Nature (London)* **377,** 62–65.
30. Kasai, H. (1999) *Trends Neurosci.* **22,** 88–93.
31. Bi, G., Alderton, J. M. & Steinhardt, R. A. (1995) *J. Cell Biol.* **131,** 1747–1758.
32. Terasaki, M., Miyake, K. & McNeil, P. L. (1997) *J. Cell Biol.* **139,** 63–74.
33. Passafaro, M., Rosa, P., Sala, C., Clementi, F. & Sher, E. (1996) *J. Biol. Chem.* **271,** 30096–30104.